

26531

## Bayesian Inversion of Time-lapse Seismic Data using Bimodal Prior Models

I. Amaliksen\* (Statoil ASA) & H. Omre (Norwegian University of Science and Technology)

### SUMMARY

---

The objective is to make inference about reservoir properties from seismic reflection data. The inversion problem is cast in a Bayesian framework, and bi-modal prior models are defined in order to honor the bi-modal behavior of the saturation variable. By using a Gauss-linear likelihood model the explicit expressions for the posterior models are obtained by the convenient properties of the family of Gaussian distributions. The posterior models define computationally efficient inversion methods that can be used to make predictions of the reservoir variables while providing an uncertainty assessment. The inversion methodologies are tested on synthetic seismic data with respect to porosity and water saturation at two time steps. Encouraging results are obtained under realistic signal-noise ratios.

## Introduction

Inversion of time-lapse seismic AVO data appears increasingly important during the life time of a reservoir. The matrix response is usually dominating the fluid response in the data, hence formal models are needed in order to obtain reliable fluid inversion results. The bi-modal behaviour of the saturation variable causes particular problems. Consider a profile through a sandstone reservoir discretized into  $(1, \dots, n, \dots, N)$ . The objective is to predict the reservoir time-constant porosity  $\phi$  and the time-varying water saturation  $s_w$  along the profile at two points in time,  $\mathbf{r}_t = (\phi, s_{wt})$  at  $t = (t_0, t_1)$ . Histograms of the reservoir variables from a comparable profile is displayed in Figure 1. Time-lapse seismic AVO profiles for three angles are available at the two times,  $\mathbf{d}_t = (\mathbf{d}_t^0, \mathbf{d}_t^{15}, \mathbf{d}_t^{30})$ . We also introduce a set of support variables at each  $t$ ;  $\mathbf{m}_t = (\mathbf{v}_{pt}, \mathbf{v}_{st}, \rho_t)$  being the elastic material properties. In the modelling we use logit-transformed reservoir variables and log-transformed elastic properties.

## Model

The assessment of the reservoir variables given the seismic AVO data is made by Bayesian inversion, hence the posterior model is:

$$[\mathbf{r}_t | \mathbf{d}_t] \rightarrow p(\mathbf{r}_t | \mathbf{d}_t) = [p(\mathbf{d}_t)]^{-1} \times p(\mathbf{d}_t | \mathbf{r}_t) p(\mathbf{r}_t),$$

with  $p(\mathbf{d}_t | \mathbf{r}_t)$  and  $p(\mathbf{r}_t)$  being the likelihood and prior models, respectively.

The likelihood models for the seismic AVO data given the elastic properties, see Buland and Omre (2003), and the elastic properties given the reservoir variables, see Landrø (2001), are:

$$\begin{aligned} [\mathbf{d}_t | \mathbf{m}_t] &= \mathbf{WADm}_t + \epsilon_t^{d|m} \rightarrow p(\mathbf{d}_t | \mathbf{m}_t) = \phi_{3N}(\mathbf{d}_t; \mathbf{WADm}_t, \Sigma_{d|m}), \\ [\mathbf{m}_t | \mathbf{r}_t] &= \mathbf{Br}_t + \epsilon_t^{m|r} \rightarrow p(\mathbf{m}_t | \mathbf{r}_t) = \phi_{3N}(\mathbf{m}_t; \mathbf{Br}_t, \sigma_{m|r}^2 \mathbf{I}_{3N}), \end{aligned}$$

where  $\mathbf{W}$  is the wavelet matrix,  $\mathbf{A}$  is the linearized Zoeppritz approximation matrix,  $\mathbf{D}$  is the differential matrix and  $\epsilon_t^{d|m}$  is a colored Gaussian error term. Moreover,  $\mathbf{B}$  is the linearized rock physics model, which is displayed in Figure 2-4. Note that the response from the porosity dominates the fluid response. The corresponding likelihood for seismic AVO data given the reservoir variables of interest is:

$$[\mathbf{d}_t | \mathbf{r}_t] \rightarrow p(\mathbf{d}_t | \mathbf{r}_t) = \phi_{3N}(\mathbf{d}_t; \mathbf{WADBr}_t, \sigma_{m|r}^2 [\mathbf{WAD}][\mathbf{WAD}]^T + \Sigma_{d|m}).$$

Hence the likelihood for the difference in the time-lapse seismic AVO data given the change in reservoir variables is:

$$[\Delta_{01}\mathbf{d} | \Delta_{01}\mathbf{r}] \rightarrow p(\Delta_{01}\mathbf{d} | \Delta_{01}\mathbf{r}) = \phi_{3N}(\Delta_{01}\mathbf{d}; \mathbf{WADB}\Delta_{01}\mathbf{r}, [\mathbf{WAD}]\Sigma_{m|r}^{01}[\mathbf{WAD}]^T + \Sigma_{d|m}^{01}),$$

where  $\Sigma_{\cdot}^{01}$  are temporal covariance matrices for the error terms which may be complicated to identify. Note that  $\Delta_{01}\mathbf{r} = (0i_N, \Delta_{01}s)$  since the porosity is time constant.

A prior Gaussian model is normally assumed for mathematical convenient reasons, see Buland and Omre (2003):

$$\mathbf{r}_t \rightarrow p(\mathbf{r}_t) = \phi_{2N}(\mathbf{r}_t; \mu_r i_{2N}, \Sigma_r),$$

despite that the marginal uni-modal Gauss pdf would not represent the bi-modal saturation histogram in Figure 1 very well. Alternative, mathematically tractable prior models exists, however:

The prior Generalized Gaussian model, see Rimstad and Omre (2012), is defined as:

$$\begin{aligned} \mathbf{r}_t \rightarrow p(\mathbf{r}_t) &= \left[ \Phi_{2N}(\cup_{n=1}^{2N} \Psi_v; 0i_{2N}, \tau_v^2 \Sigma_s^\rho + (1 - \tau_v^2) \mathbf{I}_{2N}) \right]^{-1} \\ &\times \prod_{n=1}^{2N} \Phi_1(\Psi_v; \tau_v [\sigma_s]^{-1} (r_{nt} - \mu_s), 1 - \tau_v^2) \phi_{2N}(\mathbf{r}_t; \mu_s i_{2N}, \sigma_s^2 \Sigma_s^\rho), \end{aligned}$$

where  $\Phi_n(\Psi; \mu, \Sigma)$  is the probability that  $\{x \in \Psi\}$  for  $x \rightarrow \phi_n(x; \mu, \Sigma)$ , and with  $\mu_s$  and  $\sigma_s^2$  being location and scale parameters respectively. Further,  $\Sigma_s^\rho$  is a spatial correlation matrix, while  $\tau_v$  and the set  $\Psi_v \in \mathcal{R}^1$  are shape parameters. The corresponding marginal pdf may be multi-modal, skewed and/or heavitailed, see Figure 5a.

The prior Mixture Gaussian model, see Grana and Della Rossa (2010), is defined as:

$$\mathbf{r}_t \rightarrow p(\mathbf{r}_t) = \sum_{\boldsymbol{\kappa} \in \Omega_{\boldsymbol{\kappa}}^N} \phi_{2N}(\mathbf{r}_t; \boldsymbol{\mu}_{r|\boldsymbol{\kappa}}, \boldsymbol{\Sigma}_{r|\boldsymbol{\kappa}}^\sigma \boldsymbol{\Sigma}_r^\rho \boldsymbol{\Sigma}_{r|\boldsymbol{\kappa}}^\sigma) p(\boldsymbol{\kappa}),$$

with  $\boldsymbol{\kappa} = (\kappa_1, \dots, \kappa_n, \dots, \kappa_N)$  being the mode indicator vector with  $\kappa_n \in \Omega_{\kappa} : \{1, \dots, K\}$ , and  $\boldsymbol{\mu}_{r|\boldsymbol{\kappa}}$  and  $\boldsymbol{\Sigma}_{r|\boldsymbol{\kappa}}^\sigma$  being mode-dependent expectation vector and diagonal standard deviation matrix, respectively, while  $\boldsymbol{\Sigma}_r^\rho$  is the spatial correlation matrix. The mode indicator is assigned the prior model  $p(\boldsymbol{\kappa}) = \prod_{n=1}^N p(\kappa_n)$ . The corresponding marginal pdf can be multi-modal, see Figure 5b.

The posterior model  $p(\mathbf{r}_t | \mathbf{d}_t)$  is defined by the Gauss-linear likelihood model and one of the three alternative prior models, Gauss, Gen-Gauss or Mix-Gauss. Note that the Gauss prior model appears as a special case for both the other prior models. The Gaussian marginal pdf is represented with a stippled line in Figure 5a-b. Bayesian Gen-Gauss inversion is analytically tractable, see Rimstad and Omre (2014). For Bayesian Mix-Gauss inversion a reliable approximate solution can be assessed, and simulations from the exact solution can be obtained by an indep-prop MCMC algorithm, see Rimstad and Omre (2012).

### Example

Consider the reference porosity/water saturation profiles from times  $t = (t_0, t_1)$  in Figure 6. The profile at  $t_0$  is real and represents oil with two water zones with tops at approximate depths 20 and 90, while the synthetic profile at  $t_1$  indicates that water has replaced oil at top of these two zones. The corresponding synthetic seismic AVO data by using the Gauss-linear forward model with  $S/N = 2$  is presented in Figure 7. The Gauss, Gen-Gauss and Mix-Gauss prior models are assigned model parameters to reproduce the marginal pdfs in Figure 1. The two latter reproduces the bi-modality in water saturation. A relatively continuous spatial correlation function is used, see Amalixsen (2014) for more details.

The posterior model for  $[\mathbf{r}_0 | \mathbf{d}_0]$  is assessed directly, while the posterior for  $[\mathbf{r}_1 | \mathbf{d}_0, \mathbf{d}_1]$  is assessed through saturation changes by the difference likelihood model. The MAP predictions based on the three posterior models with varying prior models, is co-displayed with the reference profiles in Figure 8-10. The porosity predictions are very similar due to the uni-modal characteristics of porosity in this example. For water saturation at  $t_0$ , the prediction from Bayesian Gauss inversion is severely regressed towards the constant prior expectation profile. Predictions from Bayesian Gen-Gauss and Mix-Gauss inversion flip clearly between the modes of the saturation distribution - as preferred. The modes appears to be somewhat too far apart, though. Note, however, that if the predictions are judged by a MSE criterion, see Table 1, the Gauss prior model is favorable - which may be misleading.

### Conclusion

Bayesian inversion with a Gauss-linear likelihood model and bi-modal prior models are defined. These models capture the bi-modal characteristics of the saturation. The inversion is demonstrated on a synthetic time-lapse seismic AVO inversion case. Encouraging results are obtained, although more formal model adaption procedures should be worked out.

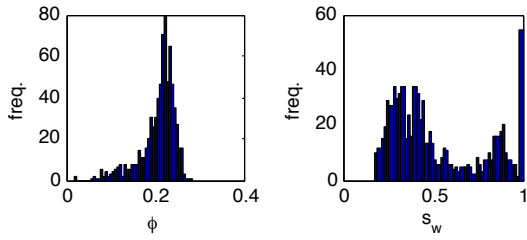


Figure 1: Histogram of porosity  $\phi$  and water saturation  $s_w$  from comparable profile.

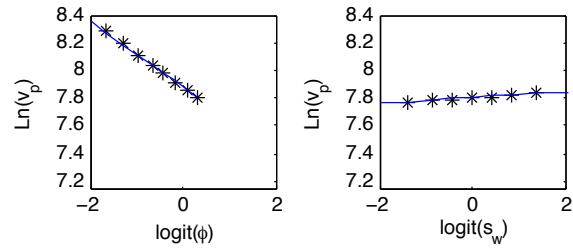


Figure 2: Linearized relation between elastic property  $v_p$  and reservoir variable ( $\phi, s_w$ ).

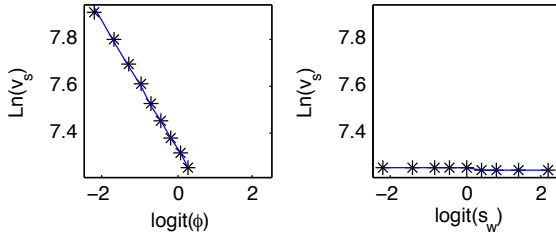


Figure 3: Linearized relation between elastic property  $v_s$  and reservoir variable ( $\phi, s_w$ ).

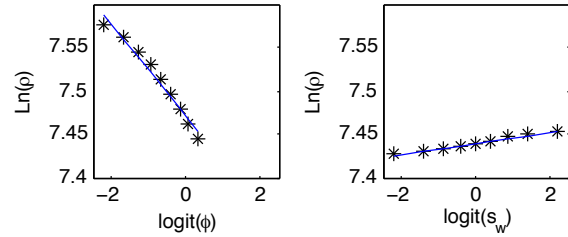


Figure 4: Linearized relation between elastic property  $\rho$  and reservoir variable ( $\phi, s_w$ ).

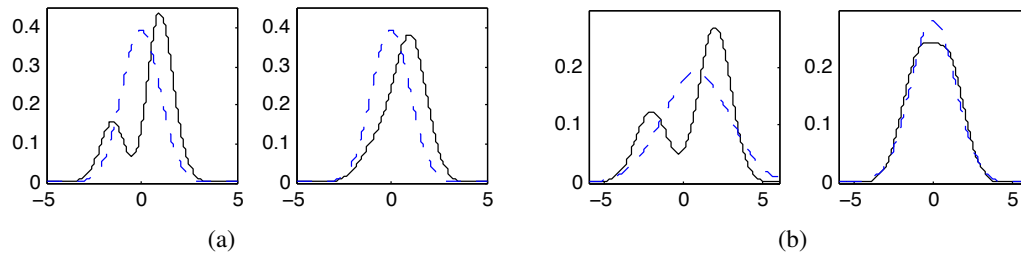


Figure 5: Examples of marginal pdfs from prior models, a) Gen-Gauss prior b) Mix-Gauss prior.

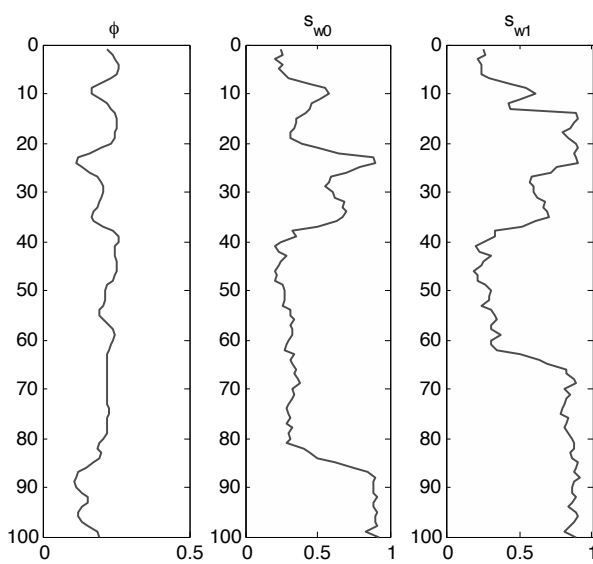


Figure 6: Synthetic reference seismic AVO data ( $d_0, d_1$ )

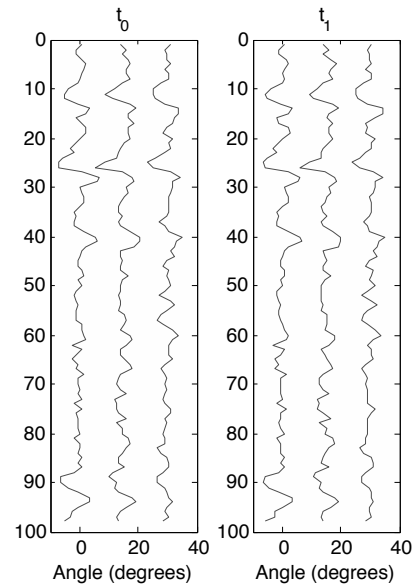
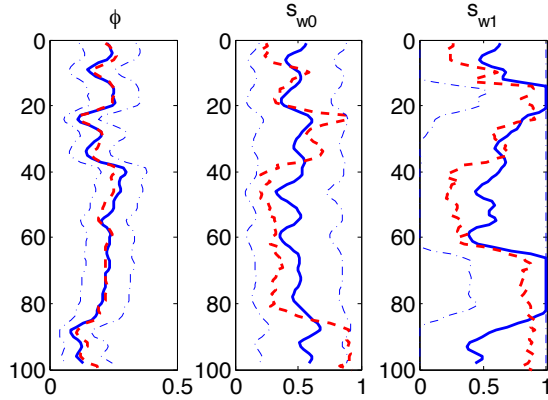


Figure 7: Reference reservoir variable profile, ( $\phi, s_{w0}$ ) real profiles,  $s_{w1}$  synthetic profile



Prior	$\phi$	$s_{w0}$	$s_{w1}$
Gauss	0.02	0.17	0.15
GenGauss	0.02	0.18	0.20
MixGauss	0.02	0.14	0.22

Table 1: Bayesian inversion results. RMS-error in the max mode predictor for varying prior models.

Figure 8: Bayesian Gauss inversion results. Reference profile (hatch), max-mode predictor (solid) and 95%-prediction interval (dot-hatch)

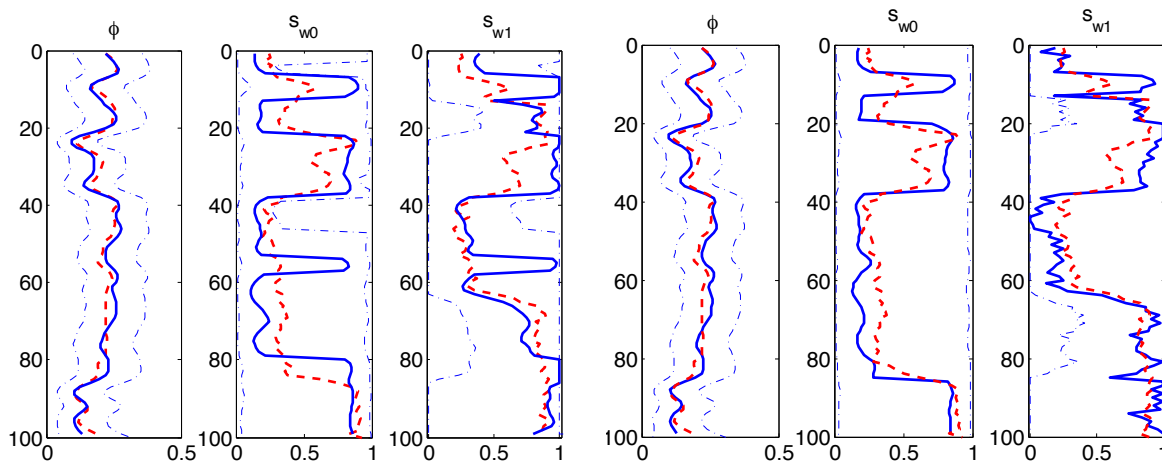


Figure 9: Bayesian Gen-Gauss inversion results. Reference profile (hatch), max-mode predictor (solid) and 95%-prediction interval (dot-hatch)

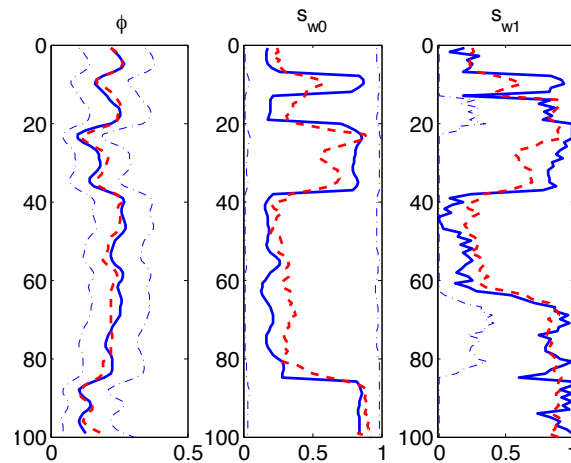


Figure 10: Bayesian Mix-Gauss inversion results. Reference profile (hatch), max-mode predictor (solid) and 95%-prediction interval (dot-hatch)

## References

- Amalixsen, I. [2014] *Bayesian Inversion of Time-lapse Seismic Data using Bimodal Prior Models*. Master's thesis, Norwegian University of Science and Technology- Department of Mathematical Sciences.
- Buland, A. and Omre, H. [2003] Bayesian linearized AVO inversion. *Geophysics*, **68**(1), 185–198.
- Grana, D. and Della Rossa, E. [2010] Probabilistic petrophysical-properties estimation integrating statistical rock physics with seismic inversion. *Geophysics*, **75**(3), O21–O37.
- Landrø, M. [2001] Discrimination between pressure and fluid saturation changes from time-lapse seismic data. *Geophysics*, **66**(3), 836–844.
- Rimstad, K. and Omre, H. [2012] Approximate posterior distributions for convolved two-level hidden Markov models. *Computational Statistics and Data analysis*, **58**, 187–200.
- Rimstad, K. and Omre, H. [2014] Generalized Gaussian Random Fields using hidden sections. *arXiv:1402.1144 [stat.ME]*.